

Article

Cardiac Toxicity Induced by Long-Term Environmental Levels of MC-LR Exposure in Mice

Canqun Yan ^{1,†}, Ying Liu ^{2,†}, Yue Yang ³, Isaac Yaw Massey ², Linghui Cao ⁴, Muwaffak Al Osman ³ and Fei Yang ^{2,3,5,*} 

- ¹ Department of Health Management Center, The Second Affiliated Hospital, Hengyang Medical School, University of South China, Hengyang 421009, China; 1992020003@usc.edu.cn
- ² Hunan Province Key Laboratory of Typical Environmental Pollution and Health Hazards, School of Public Health, Hengyang Medical School, University of South China, Hengyang 421009, China; liuying@usc.edu.cn (Y.L.); mriymassey@csu.edu.cn (I.Y.M.)
- ³ Hunan Provincial Key Laboratory of Clinical Epidemiology, Xiangya School of Public Health, Central South University, Changsha 410017, China; yangy930806@126.com (Y.Y.); 206911027@csu.edu.cn (M.A.O.)
- ⁴ Changsha Central Hospital, Changsha 410004, China; ch223234@126.com
- ⁵ Laboratory of Ecological Environment and Critical Human Diseases Prevention of Hunan Province, School of Basic Medical Sciences, Hengyang Medical School, University of South China, Hengyang 421009, China
- * Correspondence: phfyang@usc.edu.cn
- † These authors contributed equally to this work.

Abstract: Cyanobacterial blooms are considered a serious global environmental problem. Recent studies provided evidence for a positive association between exposure to microcystin-LR (MC-LR) and cardiotoxicity, posing a threat to human cardiovascular health. However, there are few studies on the cardiotoxic effects and mechanisms of long-term low-dose MC-LR exposure. Therefore, this study explored the long-term toxic effects and toxic mechanisms of MC-LR on the heart and provided evidence for the induction of cardiovascular disease by MC-LR. C57BL/6 mice were exposed to 0, 1, 30, 60, 90, and 120 µg/L MC-LR via drinking water for 9 months and subsequently necropsied to examine the hearts for microstructural changes using H&E and Masson staining. The results demonstrated fibrotic changes, and qPCR and Western blots showed a significant up-regulation of the markers of myocardial fibrosis, including TGF-β1, α-SMA, COL1, and MMP9. Through the screening of signaling pathways, it was found the expression of PI3K/AKT/mTOR signaling pathway proteins was up-regulated. These data first suggested MC-LR may induce myocardial fibrosis by activating the PI3K/AKT/mTOR signaling pathway. This study explored the toxicity of microcystins to the heart and preliminarily explored the toxic mechanisms of long-term toxicity for the first time, providing a theoretical reference for preventing cardiovascular diseases caused by MC-LR.

Keywords: microcystins; chronic toxicity; myocardial fibrosis; PI3K/AKT/mTOR signaling pathway

Key Contribution: Long-term environmental MC-LR exposure induced myocardial fibrosis, which is mediated via PI3K/AKT/mTOR signaling pathway.



Citation: Yan, C.; Liu, Y.; Yang, Y.; Massey, I.Y.; Cao, L.; Osman, M.A.; Yang, F. Cardiac Toxicity Induced by Long-Term Environmental Levels of MC-LR Exposure in Mice. *Toxins* **2023**, *15*, 427. <https://doi.org/10.3390/toxins15070427>

Received: 12 July 2022
Revised: 31 May 2023
Accepted: 13 June 2023
Published: 30 June 2023



Copyright: © 2023 by the authors. Licensee MDPI, Basel, Switzerland. This article is an open access article distributed under the terms and conditions of the Creative Commons Attribution (CC BY) license (<https://creativecommons.org/licenses/by/4.0/>).

1. Introduction

Globally, increased eutrophication of water bodies and the proliferation of cyanobacteria have become a major public health issue. Cyanobacterial blooms are typically characterized by the massive formation of cyanobacteria and diatoms, which resulted in hypoxia and a bad smell. In addition, cyanobacteria such as *Microcystis*, *Anabaena*, *Arabidopsis*, *Oscillatoria*, and *Nostoc* [1] produce various potent toxins such as cyclic peptides, alkaloids, and lipopolysaccharides during their metabolism [2]. Exposure to these toxins has negative effects on human and animal health [3]. Among the cyanobacterial toxins produced during outbreaks of cyanobacterial blooms, monocyclic peptide MCs are the most abundant,

widely distributed, highly toxic, and difficult to remove after being dissolved in water [4–6]. Therefore, the consequences of MCs on the environment, humans, and animals have attracted much attention in research. At least 279 MC variants have been documented, with MC-LR being the most toxic [7,8]. Human exposure to MCs can occur through various routes, including ingestion of ‘contaminated’ water during hemodialysis, consumption of drinking water, physical contact with the water, and engaging in recreational activities in waterbodies during algal blooms. However, drinking water remains the main route of exposure [3]. Studies have shown that MC-LR plays a critical role in damaging organ cells under both acute and chronic exposure. The liver [9,10], kidney [11–13], nervous system [14], gastrointestinal tract [15,16], reproductive system [17–19], and cardiovascular system [20,21] have been reported to be the target organs for MC toxicity. To minimize the health hazards caused by MCs, the World Health Organization (WHO) recommended that the maximum allowable content of MCs in drinking water should not exceed 1 µg/L [22].

Previous research has shown MCs can be transported into various cells by the organic anion-transporting polypeptide (OATP) [23]. Several OATP family genes, including OATP4A1, OATP2A1, OATP2B1, and OATP3A1, have been reported to be expressed in cardiac tissue [24]. This infers MCs can be transported to and accumulated in cardiac tissue cells, ultimately endangering the cardiac tissue. Zhao et al. [25] found that MC-LR directly induces cardiovascular toxicity by altering the cardiomyocyte morphology, status of apoptosis and proliferation, cytoskeleton, rhythm, differential expression/activity of transcription factors, ultrastructure of cardiomyocyte mitochondrial respiratory chain, and metalloproteinase activity when rabbits were injected with 12.5 and 50 µg/kg MC-LR (equal 75 and 300 µg/L in mice [26]) for 48 h. MC-LR exposure also enhanced the production of reactive oxygen species (ROS) and endoplasmic reticulum oxidative stress, leading to cytoskeleton disruption, as well as the dysfunction of mitochondria and the endoplasmic reticulum [27]. Milutinovic et al. [28] found that MC-LR could induce the enlargement of cardiomyocytes, loss of cell cross-striations, lower myofibril volume fraction, fibrosis, and mononuclear infiltration in the interstitial tissue in male adult Wistar rats, which were gavaged every second day for 8 months with MC-LR (10 µg/kg in rats equals 1687.5 µg/L in mice). Previous studies focused on the cardiovascular toxicity of short-term high-dose MC-LR, and no studies have investigated the toxicity and mechanisms of long-term low-dose exposure to MC-LR through drinking water and its effects on the heart [29].

To date, information regarding the cardiotoxic effects of MC-LR, especially low concentration of long-term MC-LR exposure, remains limited, and the underlying mechanism is still unclear. The majority of previous investigations examined the acute effects of exposure to high-concentration MC-LR on the heart. This study is designed to explore the effects of low concentration (1, 30, 60, 90, and 120 µg/L MC-LR) MC-LR (WHO guideline 1 µg/L) following chronic exposure on the heart and to elucidate the potential mechanism of MC-LR cardiotoxicity including the involvement of the PI3K/AKT pathway according to *in vivo* experiments. The goals of this study are to further understand the mechanism of microcystin cardiotoxicity and provide a theoretical basis and new perspective on the prevention, diagnosis, and treatment of microcystin-induced cardiotoxicity.

2. Results

2.1. Detection of Endogenous Exposure to MC-LR in Cardiac Tissue

To detect the presence of internal exposure of the heart tissue to MC-LR, total heart protein was extracted, and a Western blot was performed. Except for the control group, MC-LR was detected in all MC-LR treatment groups (Figure 1). This suggests MC-LR entered the heart tissue via absorption in mice. The concentration of MC-LR increased in the heart when the oral MC-LR dose increased.

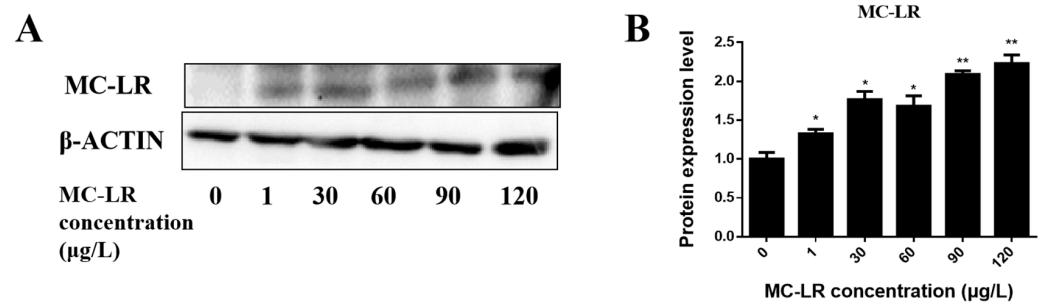


Figure 1. Detection of MC-LR in cardiac tissue. (A) Representative bands of Western blotting. (B) showed the quantitative results of MC-LR via Western blot, respectively. (* indicates a significant difference at $p < 0.05$, and ** indicates a significant difference at $p < 0.01$; $n = 3$).

2.2. The Effect of MC-LR on the General Condition and the Weight Index of the Mouse Heart

During the period of exposure, the mice's body weights were recorded every two weeks (Figure 2A). No deaths or abnormal behaviors were observed in the mice during the course of the experiment. Compared with the control group, there were no significant differences in body weight change compared to controls over the nine-month course of this study. The volume of drinking water consumed by the mice was measured each week during the exposure period (Figure 2B). In fact, the results of Figure 2A showed that the total amount of water drunk by five mice per cage was about 300 mL per month, which was equivalent to drinking 10 mL of water per day, that was, each mouse drank 2 mL of water per day. There was no significant change in the amount of drinking water consumed among the MC-LR exposure groups. The data of the drinking water and exposure doses of mice and the average daily intake of MC-LR for each mouse in each dose group were estimated (Figure 2C). The heart weights for each mouse are normalized to their body weight. The mouse heart weight index is shown that there were no significant changes in the cardiac weight index compared with the control group (Figure 2D).

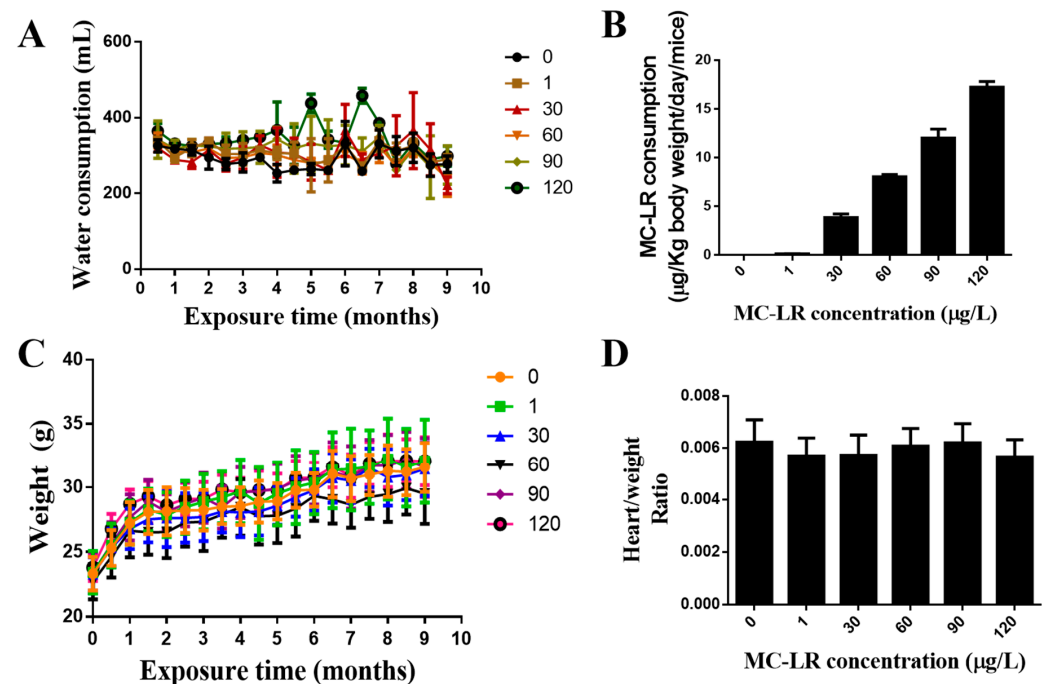


Figure 2. Changes in the consumption of water (A), the intake of MC-LR in every dose group (B), the body weight (C), and the mouse heart weight index (D), by the C57BL/6 mice during a 9-month chronic exposure to different concentrations of MC-LR ($n = 10$).

2.3. Effects of MC-LR Treatment on Mouse Cardiac Function

The results demonstrated that the heart function of mice in the highest exposure (120 µg/L) group decreased significantly. There was an absence of differences in the other treatment groups (Table 1).

Table 1. Echocardiography results (* indicates a significant difference at $p < 0.05$, ** indicates a significant difference at $p < 0.01$, and *** indicates a significant difference at $p < 0.001$; $n = 3$).

Groups	Control (µg/L)	MC-LR Treated (120 µg/L)
LVEF (%)	53.88 ± 3.96	36.28 ± 4.32 ***
LVFS (%)	27.36 ± 2.38	17.24 ± 2.39 ***
LVESD(mm)	29.4 ± 7.55	49.58 ± 2.90 **
LVEDD (mm)	63.02 ± 12.22	77.95 ± 4.43 *
LVPWd (mm)	0.57 ± 0.10	0.72 ± 0.07
LVPWs (mm)	0.88 ± 0.17	0.89 ± 0.11
IDd (mm)	3.81 ± 0.33	4.18 ± 0.10
LVIDs (mm)	2.78 ± 0.32	3.46 ± 0.08
HR (beat/min)	403.28 ± 43.69	388.00 ± 26.03

2.4. Effects of MC-LR Treatment on the Histological Morphology of Mouse Heart

The mice's exposure to MC-LR in drinking water for 9 months resulted in observed changes in cardiac histology. Cardiac micromorphology is shown in Figure 3A,B, indicating the presence of myocardial fibrosis. There was an absence of differences in the other treatment groups. To further clarify the phenotype of myocardial fibrosis, Masson staining was performed to observe the abundance of collagen-specific tissues. An increase in blue collagen fibers can be observed as a diffuse pattern of enhanced collagen interspersed between myocardial fiber bundles. There was an absence of differences in the other treatment groups (Figure 3C,D).

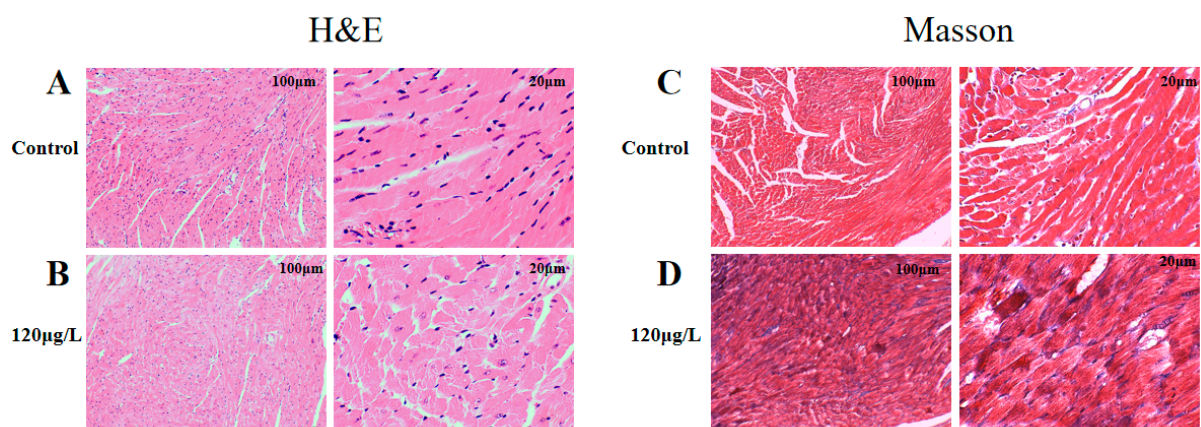


Figure 3. The effect of MC-LR treatment on the morphology of mouse nodal heart. H&E staining (A) represents the Control group; (B) represents the 120 µg/L MC-LR exposure group ($n = 3$). Masson Staining (C) represents the Control group; (D) represents the 120 µg/L MC-LR exposure group ($n = 3$). (Blue represented collagen fibers, and red represented muscle fibers and erythrocytes).

2.5. Effects of MC-LR on the Expression of Myocardial Fibrosis Marker Factors in Mouse Heart Tissue

To further clarify the myocardial fibrosis caused by MC-LR, qPCR was used to determine the presence and abundance of mRNA levels for myocardial fibrosis marker factors TGF-β1, α-SMA, and Col1. The relative levels of mRNA levels for TGF-β1, α-SMA, and

COL1 mRNA were significantly increased in all MC-LR exposure groups compared to the control group (Figure 4).

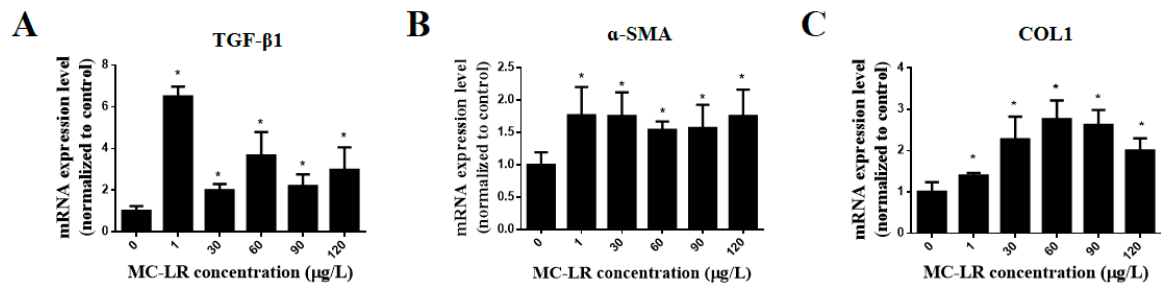


Figure 4. The expression of myocardial fibrosis factors TGF-β1 (A), α-SMA (B), and COL 1 (C) by the C57BL/6 mice during a 9-month chronic exposure to different concentrations of MC-LR. (* indicate significant difference at $p < 0.05$, $n = 3$).

In addition, changes in protein levels of these myocardial fibrosis marker factors were determined via Western blot. The results are shown in Figure 5. Compared to the control group, the protein levels of all measured cardiac fibrosis markers were significantly up-regulated at all doses of MC-LR treatment.

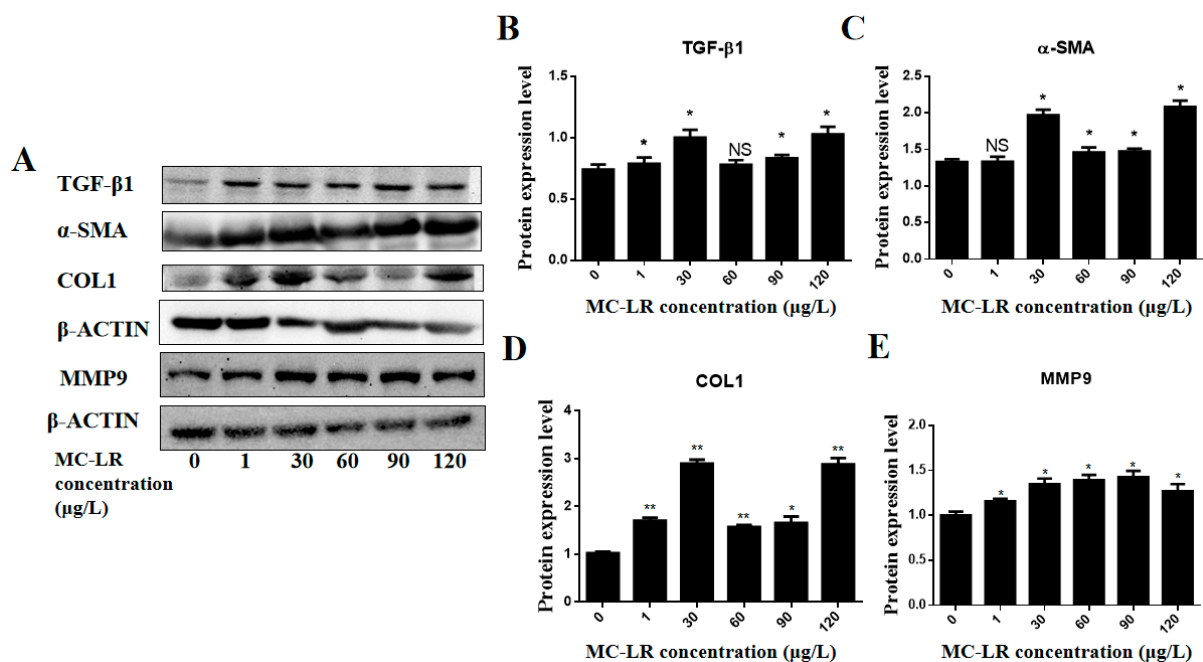


Figure 5. Western blot detection of the effect of MC-LR on the expression of myocardial fibrosis factors in mouse heart tissue. (A) represents Western blot results, and (B–E) showed the quantitative results of TGF-β1, α-SMA, COL1, and MMP9 via Western blot, respectively. (NS indicates a significant difference at $p > 0.05$, * indicates a significant difference at $p < 0.05$, and ** indicates a significant difference at $p < 0.01$; $n = 3$).

2.6. MC-LR Expression of PI3K/AKT/mTOR Pathway-Related Proteins in the Mouse Heart

To more fully elucidate the mechanism of MC-LR-induced cardiotoxicity, Western blotting was used to detect the expression levels of p-PI3K, PI3K, p-AKT, AKT, p-mTOR, and mTOR protein. Compared to the control, the relative expression of p-PI3K/PI3K protein did not change significantly in the 1 µg/L MC-LR exposure group but was significantly elevated in the 30, 60, 90, and 120 µg/L MC-LR exposure groups ($p < 0.05$) to confirm MC-LR can activate the PI3K/AKT/mTOR pathway. Similarly, compared with the control

group, the relative expression of p-mTOR/mTOR protein did not significantly change in the 1 µg/L MC-LR exposure group but was significantly elevated in the 30, 60, 90, and 120 µg/L MC-LR exposure group. The relative expression levels were all significantly increased ($p < 0.05$), as shown in Figure 6.

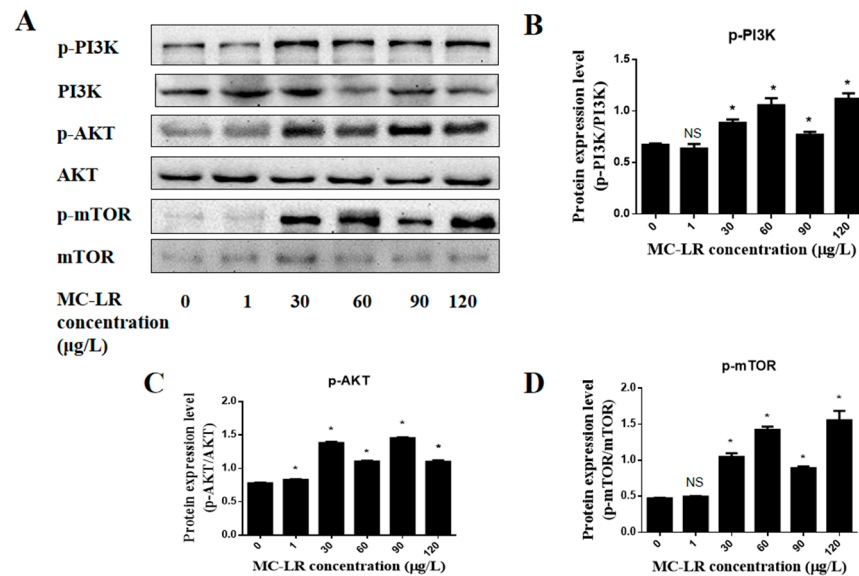


Figure 6. Effects of MC-LR on PI3K/AKT/mTOR pathway-related proteins in mouse heart tissue. (A) Related protein bands detected via Western Blot; (B–D) Statistical bar graph of protein expression of p-PI3K, p-AKT and p-mTOR. (NS indicates a significant difference at $p > 0.05$, and * indicates a significant difference at $p < 0.05$, $n = 3$).

3. Discussion

This present study investigated the effects of MC-LR on the heart using a chronic oral exposure regimen administered in a dosimetric fashion. The heart tissues were examined for internal exposure dosing after 9 months of oral MC-LR exposure. As anticipated, except for the control group, algal toxins were detected in all MC-LR-treated groups. H&E and Masson's staining were applied to observe the microstructure of the heart, while changes in mRNA expression levels and protein levels in myocardial fibrosis-related factors were measured.

Mice demonstrated 100% survival following 9 months of MC-LR treatment. No significant differences in body weight gain, diet, water consumption, or activity levels were observed. No abnormality in the heart weight ratio between the MC-LR-treated group and the control group was noted. Du et al. [30] treated mice with low-dose MC-LR for one month without significant changes in body weight; these results are consistent with our results. The findings of this study showed that chronic exposure to MC-LR could decrease heart function in mice, and this study is likely the first or among the first to demonstrate such a decrease. To date, there is no research showing MC-LR leads to a decline in heart function. Previous research shows MC-LR suppressed heart rate. For example, Qiu et al. [31] injected MC-LR with high concentrations of 0.16 LD₅₀ (14 g/kg) and 1LD₅₀ (87 g/kg), and there is a drop in heart rate and blood pressure in survival rats [31]. Martins et al. [32] injected 100 µg/kg MC-LR into *Hoplias malabaricus* induced cytotoxicity by enhancing the activity of oxidative stress and other related enzymes. Saraf et al. [33] found that MC-LR can suppress the heart rate of *Oryzias Latipes*. Qi et al. [34] found that zebrafish (*Danio rerio*) larvae had morphological deformations, growth retardation, heart rate inhibition, and increased apoptosis after 96 h of treatment with 4.0 mM MC-LR. In contrast, the results of this study found the heart rate of the mice in all MC-LR treatment groups was not significantly different from that of the control group (Table 1). Interestingly, this present research first found MC-LR changed heart function, including LVEF, LVFS,

LVESD, and LVEDD. These differences in the findings suggested that there may be some differences in the toxic mechanism of acute and chronic exposure to MC-LR, as well as differences in concentrations of MC-LR. In the future, the heart rate of the other lower treatment group (1, 30, 60, and 90 $\mu\text{g/L}$) will be further performed to reveal the heart function in mice.

Milutinovic et al. [28] found that the appearance and morphology of the heart of animals treated with MC-LR did not change significantly for eight months. TUNEL staining showed no change in apoptosis, but the cytoskeleton structure of cardiomyocytes was destroyed, with myocyte striations absent and myofibril volume fraction reduced. Further observations were an increase in cardiomyocyte volume, a decrease in the volume of myofibrils, and the presence of fibrosis, along with monocyte infiltration in the interstitial tissues of the heart [28]. Suput et al. [35] used MC-LR to conduct a similar chronic toxicity study and demonstrated a reduction in the volume and density of the myocardium, accompanied by fibrous proliferation and limited infiltration of lymphocytes. These findings indicated MC-LR can induce myocardial fibrosis, which is consistent with ours.

Cardiac fibrosis is a common pathological change in many advanced cardiovascular diseases, including ischemic heart disease, hypertension, and heart failure. Myocardial fibrosis can affect cardiac function by increasing myocardial stiffness and impairing conduction, which have been identified as common risk factors for heart failure and arrhythmias [36]. Cells in the heart express profibrotic factors, cytokines, and chemokines, such as α -SMA, TGF- β 1, and COL1 after stimulation by profibrotic factor signals and cardiac injury. These factors bind to their corresponding receptors and activate signaling pathways that regulate cardiac fibrosis [37]. Furthermore, once profibrotic growth factors are secreted in fibroblasts of the heart, these factors form a positive feedback regulation, which, in turn, amplifies the fibrotic signal and ultimately promotes the development of cardiac fibrosis [25]. Fibroblasts make up the majority of mammalian heart cells, and they are primarily responsible for the production of major components of the extracellular matrix, including COL (I, III, V, and VI) and fibronectin. MMP-9 can be used as a marker for serious changes in the heart and would be associated with inflammation and fibrosis, which was over-expression in this present study [38]. The occurrence of myocardial fibrosis can pose a serious threat to human health. However, information regarding the cardiotoxic effects of MC-LR, especially low concentration of long-term MC-LR exposure, remains limited, and the underlying mechanism is still unclear. This study first demonstrated that long-term low concentrations of MC-LR (120 $\mu\text{g/L}$) exposure can induce myocardial fibrosis in mice.

The PI3K/AKT signal pathway is a family of key enzymes involved in various biological processes, including cell survival, apoptosis, metastasis, differentiation, metabolism, protein synthesis, cell polarity, and motility, as well as vesicle transport and cardiac function [39]. Numerous studies have shown that PI3K is involved in the process of cardiac fibrosis. Data from a previous study [40] demonstrated that enhancing the PI3K α signal modulates, including TGF- β , and miR-21 expression, further protected cardiac fibrosis in pathological hypertrophy [41]. Ma et al. [42] found that overexpression of AKT reduces piperine-mediated protection of cardiac fibroblasts. Inhibition of AKT significantly reduces pressure-load-induced cardiac fibrosis [43]. mTOR is a direct substrate of AKT kinase. Finckenberg et al. [44] found that when the mTOR pathway was blocked, the expression levels of pro-fibrotic factors such as connective tissue growth factor, TGF- β 1, and Col3 were significantly down-regulated. These studies suggested that the PI3K/AKT/mTOR signal pathway may be involved in the regulation of cardiac fibrosis.

PI3K may regulate fibrosis by affecting myocardial contractility [45]. AKT, also known as protein kinase B (PKB), is a serine ser/threonine protein kinase that regulates cellular functions, including survival, growth, and metabolism [46]. Over-expression of AKT1 and AKT3 resulted in increased cardiomyocyte size and enhanced function [47]. Mitra et al. [48] found that OSI-027, an mTOR inhibitor, inhibited the expression of TGF- β -induced myocardial fibrosis marker factors α -SMA, Col I and Col III. The study of Liu et al. showed the PI3K/AKT signaling pathway was activated in the HL7702 cell line under the induction

of MC-LR but not in a dose or time-dependent fashion [49]. Chen et al. also found the PI3K/AKT signaling pathway was activated in testes but not in a dose-time-dependent manner [50]. In addition, the proteomics data from Zhou [51] also found that the PI3K/AKT signaling pathway was activated in the testis. The results of these studies are consistent with this current study's findings.

To further study the mechanism of MC-LR-induced myocardial fibrosis in mice, the signaling pathway was examined. It was found that MC-LR can up-regulate the expression of phosphorylated PI3K, AKT, and mTOR to activate the PI3K/AKT signaling pathway (Figure 7). Phosphorylated PI3K and phosphorylated mTOR were significantly up-regulated following 9 months of treatment at 30, 60, 90, and 120 $\mu\text{g/L}$ of MC-LR. There was no significant change in the 1 $\mu\text{g/L}$ dose group. Phosphorylated AKT was significantly up-regulated in all MC-LR treatment groups. However, the change in protein levels of these signaling molecules was not dose dependent. The potential reason is the low dose (1 $\mu\text{g/L}$) of MC-LR is insufficient to cause changes in protein levels, or the changes caused do not attain the threshold of detection. At higher concentrations (30 $\mu\text{g/L}$, 60 $\mu\text{g/L}$, 90 $\mu\text{g/L}$, and 120 $\mu\text{g/L}$), MC-LR may trigger protection mechanisms to elicit change. The mutual antagonism of toxic effects resulted in the alteration of the amount of protein, although not in a dose-response relationship. The specific mechanism remains to be further studied and elucidated.

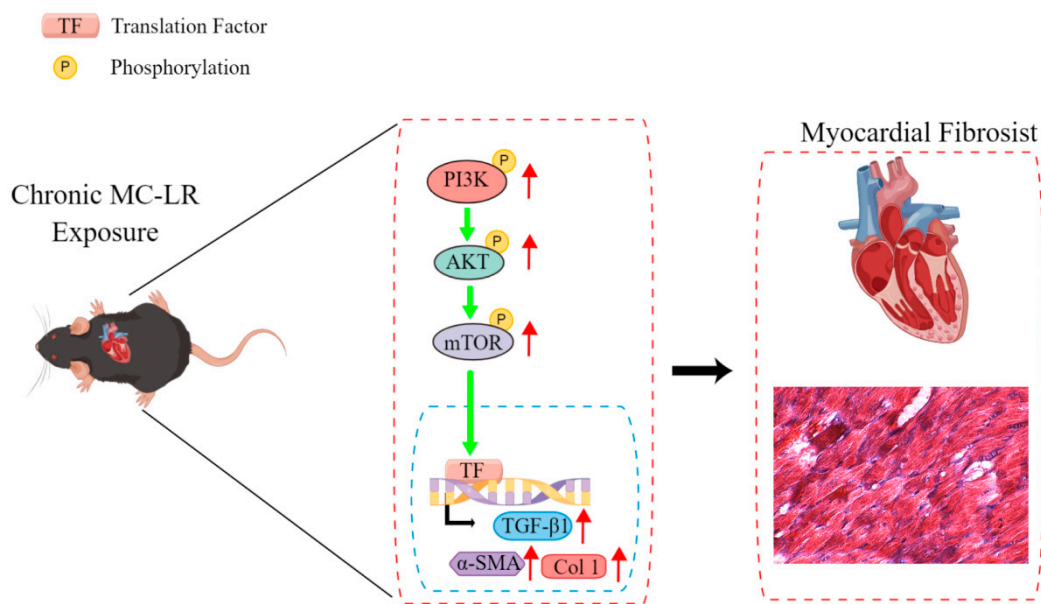


Figure 7. Long-term environmental levels of MC-LR exposure induced myocardial fibrosis through the PI3K/AKT/mTOR signaling pathway (red arrows indicate the elevated expression, and green arrows indicate the activation).

4. Conclusions

In summary, we first demonstrated that MC-LR may induce myocardial fibrosis by activating the PI3K/AKT/mTOR signaling pathway. This study explored the toxicity of microcystins to the heart and preliminarily explored the toxic mechanisms of long-term toxicity for the first time, which provides a theoretical reference for the prevention of cardiovascular diseases caused by MC-LR.

5. Materials and Methods

5.1. Materials

Grouping and Handling of Experimental Mice

Sixty specific pathogen-free (SPF) C57BL/6 male mice, 6–8 weeks of age and weighing 18–22 g, were purchased from the Hunan Slack Laboratory Animal Company and raised

in the Animal Center of the Xiangya School of Public Health at Central South University. Animal housing conditions were maintained at an ambient temperature of 21–22 °C, humidity of 75 ± 5%, and kept on a 12 h light/dark cycle. Clean rodent pellets and drinking water were provided to allow mice to eat and drink freely. Following two weeks of adaptive feeding, the mice were divided into 6 groups, based on the method of random number generation, with each group consisting of 10 mice. For each group, mice were housed in 2 cages, 5 mice per cage. MC-LR (purity ≥ 95%) was obtained from Alexis Corporation (Lausen, Switzerland) and stored at −20 °C. The MC-LR is first dissolved in DMSO and then diluted into water. Animals were provided drinking water with 0, 1, 30, 60, 90, or 120 µg/L MC-LR. The drinking water with MC-LR was changed every week. The MC-LR concentrations of drinking water were measured before and after feeding by HPLC and were not changed. Documentation was made weekly of the volume of drinking water consumed. Food was also provided promptly, adequately supplied, and freely available. Mouse body weight was measured every two weeks. The exposure time was for a total time of 9 months [30]. All animal studies were approved by the Ethics Research Committee of the Xiangya School of Public Health, Central South University (approval number, XYGW-2018-41, and date of approval: 10 November 2018).

5.2. Experimental Method

5.2.1. H&E Staining

The C57BL/6 mouse hearts were quickly removed, washed with pre-cooled saline, and immediately fixed in 4% paraformaldehyde overnight. Hearts (1/3 of the heart) were subsequently embedded in paraffin and cut into 4µm thick sections. Tissue sections were dewaxed using xylene and ethanol, washed with distilled water, and stained with hematoxylin stain to visualize the cell nucleus and intranuclear proteins for 5–15 min. Excess dye was washed from each slide with distilled water. Additionally, 1% hydrochloric acid was used for 10 s to further stain the nucleus. All slides were rinsed with running tap water for 15–30 min. A saturated solution of lithium carbonate was used to form a temporary alkalization condition to enhance the blue staining of the nucleus for all cells. After washing with distilled water, the heart sample was stained with eosin dye solution for 1–5 min and then placed in different concentrations of alcohol for dehydration. After drying at room temperature, all sections were coverslipped with a neutral mounting medium resin. Morphological changes were observed under a microscope, and images were obtained and analyzed. Each test group consisted of heart tissues from 5 mice of the different treatment groups.

5.2.2. Masson Staining

Paraffin sections were placed in xylene for 15 min for deparaffinization, followed by a graded series of ethanol (100, 90, 85%) and final rinsing with distilled water for 2 min. Tissue sections were placed in boudin solution at 56 °C for 1 h, rinsed with running water, followed by placement in lapis lazuli blue dye solution for 5 min, hematoxylin staining for 5 min, rinsed with water, treated with 1% hydrochloric acid alcohol, followed by rinsing with water. Tissue sections were subsequently placed in ponceau acid fuchsin dye solution, rinsed, and serially treated with 1% phosphomolybdic acid, bright green, 1% glacial acetic acid, and a graded series of ethanol (95, 100%) and xylenes, before coverslipping with neutral resin mounting media. This procedure stains collagen fibers blue and muscle fibers red.

5.2.3. Echocardiography

Echocardiography was performed using a Vevo 2100 ultra-high resolution small animal ultrasound imaging system and MS-550 probe. Left ventricular long-axis view, parasternal left ventricular long-axis view, suprasternal view, and apical four-chamber view were performed. At the parasternal left ventricular long-axis view, M-mode ultrasound was used to record the motion curve of the left ventricular wall. The measured parameters

included left ventricular end-systolic diameter (LVESD), left ventricular end-diastolic diameter (LVEDD), left ventricular end-diastolic posterior wall (LVPWd), LVPWs (left ventricular end-systolic posterior wall), heart rate (HR), left ventricular end-systolic stroke volume (ESV), left ventricular end-systolic stroke volume, left ventricular end-diastolic stroke volume (EDV), and left ventricular end-diastolic stroke volume. The left ventricular short-axis shortening rate was calculated (left ventricular fraction shortening, FS %) using the following formula: $FS\% = (LVEDD - LVESD) / LVEDD \times 100\%$. The left ventricular ejection fraction (LVEF%, left ventricular ejection fraction) was also calculated using the following formula: $LVEF\% = SV \text{ (stroke volume)} / EDV \times 100\%$. Cardiac output CO (cardiac output) was determined using the following formula: $CO = ESV \times HR$. Results were recorded and analyzed three times.

5.2.4. qPCR

The heart was quickly removed from the thorax, placed on ice, and washed with pre-cooled PBS. RNA was extracted using the Trizol method following tissue homogenization. The extracted RNA was reverse transcribed to synthesize cDNA according to the instructions of the Weizan reverse transcription kit following tissue homogenization. The qPCR reaction was performed according to the steps of the Weizan fluorescence quantitative kit instructions (Table 2). The reaction conditions were 95°, 30 s pre-denaturation; followed by 95°, 10 s denaturation; and 60°, 30 s annealing/extension for a total of 40 cycles. After the cycle, the temperature was raised to 95 °C for the dissolution curve. The $2^{-\Delta\Delta Ct}$ comparison method was used to calculate the transcription fold change of target genes in each treatment group relative to the average value for the control group. Fold-change calculations were based on the following equations: $\Delta Ct = Ct \text{ (target)} - Ct \text{ (internal reference)}$, $\Delta\Delta Ct = \Delta Ct \text{ (MC-LR exposure group)} - \Delta Ct \text{ (control group)}$. GraphPad Prism software was used to create statistical graphs.

Table 2. Primer sequence required for the experiment.

Primer Name	Forward Primer	Reverse Primer
β -actin	CTAAGGCCAACCGTGAAAAG	AGGGTCCCAGACAGAAGTTG
Col1	TGTTTCAGCTTTGTGGACCTC	TCAAGCATACCTCGGGTTTC
α -SMA	CCTGAAGAGCATCCGACACT	TACGTCCAGAGGCATAGAGG
TGF- β	ACCGGAGAGCCCTGGATA	CCACGTAGTAGACGATGG

5.2.5. Western Blot

At necropsy, the heart was quickly removed, placed on ice, washed with cold PBS, and dissolved in the RIPA lysis buffer (1 mL with 10 μ L protease inhibitor) at 100 mg/mL. The sample was ground in a homogenizer for 180 s at 70 hertz (HZ) and centrifuged at 12,000 rpm (4 °C) for 15 min to prepare the tissue supernatant. Total protein concentration was determined according to the BCA method. Proteins were separated by 10% SDS-PAGE gel, transferred to Polyvinylidene Fluoride (PVDF) membrane, and blocked with 5% BSA and non-fat dry milk for 1 h at room temperature. The PVDF membrane was placed in the corresponding primary antibody incubation solution prepared in advance and incubated at 4 °C overnight (Table 3). A secondary antibody solution was applied for 1 h. ECL developer solution and a chemiluminescence imager were used, and the gray value of protein bands was analyzed using Image J software.

Table 3. Antibodies and sources required for experiments.

Antibody Name	Source	Dilution Ratios
TGF- β	Proteintech, Wuhan, China	1:1000
α -SMA	Proteintech, Wuhan, China	1:1000
COL1	Proteintech, Wuhan, China	1:1000
PI3K	Proteintech, Wuhan, China	1:1000
P-PI3K	Cell Signaling Technology Company, Danvers, MA, USA	1:1000
AKT	Proteintech, Wuhan, China	1:1000
P-AKT	Cell Signaling Technology Company, Danvers, MA, USA	1:1000
mTOR	Proteintech, Wuhan, China	1:1000
p-mTOR	Proteintech, Wuhan, China	1:1000
β -ACTIN	Cell Signaling Technology Company, Danvers, MA, USA	1:1000
Rabbit secondary antibody	Abbkine company, Wuhan, China	1:3000
MC-LR	Alexis Corporation (Lausen, Switzerland)	1:3000
MMP9	Proteintech, Wuhan, China	1:1500

5.2.6. Statistical Analysis

SPSS 25 software was used for the statistical analysis of data. Two independent sample *t*-tests were used for the comparison of two groups of samples. One-way analysis of variance was used for comparison among multiple groups of samples, and the LSD test was used for further pairwise comparisons. The significance of the two-sided test level was set at $\alpha = 0.05$.

Author Contributions: Conceptualization, M.A.O.; Methodology, M.A.O.; Formal analysis, Y.Y.; Data curation, Y.Y. and L.C.; Writing—original draft, Y.L.; Writing—review and editing, C.Y., Y.L. and F.Y.; Supervision, I.Y.M.; Funding acquisition, C.Y., F.Y. All authors have read and agreed to the published version of the manuscript.

Funding: This work was supported by the Hunan Province Excellent Youth Fund (2020JJ3053); the National Natural Science Foundation of China (81773393); the Key Research and Development Projects in Hunan Province (2019SK2041); the Natural Science Joint Fund of Hunan Province (2021JJ50096).

Institutional Review Board Statement: The animal study protocol was approved by the Animal Care and Use Committee of Central South University (protocol code: XYGW-2018-41 and date of approval: 2018-11-10).

Informed Consent Statement: Not applicable.

Data Availability Statement: The data presented in this study are available in this article.

Conflicts of Interest: The authors declare no conflict of interest.

References

- Merel, S.; Walker, D.; Chicana, R.; Snyder, S.; Baures, E.; Thomas, O. State of knowledge and concerns on cyanobacterial blooms and cyanotoxins. *Environ. Int.* **2013**, *59*, 303–327. [[CrossRef](#)]
- Codd, G.A.; Morrison, L.F.; Metcalf, J.S. Cyanobacterial toxins: Risk management for health protection. *Toxicol. Appl. Pharmacol.* **2005**, *203*, 264–272. [[CrossRef](#)] [[PubMed](#)]
- Massey, I.Y.; Yang, F.; Ding, Z.; Yang, S.; Guo, J.; Tezi, C.; Al-Osman, M.; Kamegni, R.B.; Zeng, W. Exposure routes and health effects of microcystins on animals and humans: A mini-review. *Toxicon* **2018**, *151*, 156–162. [[CrossRef](#)] [[PubMed](#)]
- Chen, L.; Yang, S.; Wen, C.; Zheng, S.; Yang, Y.; Feng, X.; Chen, J.; Luo, D.; Liu, R.; Yang, F. Regulation of Microcystin-LR-Induced DNA Damage by miR-451a in HL7702 Cells. *Toxins* **2019**, *11*, 164. [[CrossRef](#)]
- Yang, F.; Huang, F.; Feng, H.; Wei, J.; Massey, I.Y.; Liang, G.; Zhang, F.; Yin, L.; Kacew, S.; Zhang, X.; et al. A complete route for biodegradation of potentially carcinogenic cyanotoxin microcystin-LR in a novel indigenous bacterium. *Water Res.* **2020**, *174*, 115638. [[CrossRef](#)]
- Wei, J.; Pengji, Z.; Zhang, J.; Peng, T.; Luo, J.; Yang, F. Biodegradation of MC-LR and its key bioactive moiety Adda by *Sphingopyxis* sp. YF1: Comprehensive elucidation of the mechanisms and pathways. *Water Res.* **2023**, *229*, 119397. [[CrossRef](#)]
- Gupta, N.; Pant, S.C.; Vijayaraghavan, R.; Rao, P.V.L. Comparative toxicity evaluation of cyanobacterial cyclic peptide toxin microcystin variants (LR, RR, YR) in mice. *Toxicology* **2003**, *188*, 285–296. [[CrossRef](#)] [[PubMed](#)]
- Cai, D.; Wei, J.; Huang, F.; Feng, H.; Peng, T.; Luo, J.; Yang, F. The detoxification activities and mechanisms of microcystinase towards MC-LR. *Ecotoxicol. Environ. Saf.* **2022**, *236*, 113436. [[CrossRef](#)]

9. Ait Abderrahim, L.; Taibi, K.; Boussaid, M.; Al-Shara, B.; Ait Abderrahim, N.; Ait Abderrahim, S. Allium sativum mitigates oxidative damages induced by Microcystin-LR in heart and liver tissues of mice. *Toxicon* **2021**, *200*, 30–37. [[CrossRef](#)]
10. Zheng, S.; Yang, Y.; Wen, C.; Liu, W.; Cao, L.; Feng, X.; Chen, J.; Wang, H.; Tang, Y.; Tian, L.; et al. Effects of environmental contaminants in water resources on nonalcoholic fatty liver disease. *Environ. Int.* **2021**, *154*, 106555. [[CrossRef](#)]
11. La-Salette, R.; Oliveira, M.M.; Palmeira, C.A.; Almeida, J.; Peixoto, F.P. Mitochondria a key role in microcystin-LR kidney intoxication. *J. Appl. Toxicol.* **2008**, *28*, 55–62. [[CrossRef](#)]
12. Piyathilaka, M.A.; Pathmalal, M.M.; Tennekoon, K.H.; De Silva, B.G.; Samarakoon, S.R.; Chanthirika, S. Microcystin-LR-induced cytotoxicity and apoptosis in human embryonic kidney and human kidney adenocarcinoma cell lines. *Microbiology* **2015**, *161*, 819–828. [[CrossRef](#)]
13. Feng, S.; Deng, S.; Tang, Y.; Liu, Y.; Yang, Y.; Xu, S.; Tang, P.; Lu, Y.; Duan, Y.; Wei, J.; et al. Microcystin-LR Combined with Cadmium Exposures and the Risk of Chronic Kidney Disease: A Case-Control Study in Central China. *Environ. Sci. Technol.* **2022**, *56*, 15818–15827. [[CrossRef](#)]
14. Hu, Y.; Chen, J.; Fan, H.; Xie, P.; He, J. A review of neurotoxicity of microcystins. *Environ. Sci. Pollut. Res. Int.* **2016**, *23*, 7211–7219. [[CrossRef](#)]
15. Ito, E.; Kondo, F.; Harada, K. First report on the distribution of orally administered microcystin-LR in mouse tissue using an immunostaining method. *Toxicon* **2000**, *38*, 37–48. [[CrossRef](#)] [[PubMed](#)]
16. Yang, Y.; Wang, H.; Wang, X.; Chen, L.; Liu, W.; Cai, D.; Deng, S.; Chu, H.; Liu, Y.; Feng, X.; et al. Long-term environmental levels of microcystin-LR exposure induces colorectal chronic inflammation, fibrosis and barrier disruption via CSF1R/Rap1b signaling pathway. *J. Hazard. Mater.* **2022**, *440*, 129793. [[CrossRef](#)] [[PubMed](#)]
17. Chen, L.; Chen, J.; Zhang, X.; Xie, P. A review of reproductive toxicity of microcystins. *J. Hazard. Mater.* **2016**, *301*, 381–399. [[CrossRef](#)] [[PubMed](#)]
18. Zhang, Y.; Zhuang, H.; Yang, H.; Xue, W.; Wang, L.; Wei, W. Microcystin-LR disturbs testicular development of giant freshwater prawn *Macrobrachium rosenbergii*. *Chemosphere* **2019**, *222*, 584–592. [[CrossRef](#)]
19. Liu, H.; Zeng, X.; Ma, Y.; Chen, X.; Losiewicz, M.D.; Du, X.; Tian, Z.; Zhang, S.; Shi, L.; Zhang, H.; et al. Long-term exposure to low concentrations of MC-LR induces blood-testis barrier damage through the RhoA/ROCK pathway. *Ecotoxicol. Environ. Saf.* **2022**, *236*, 113454. [[CrossRef](#)]
20. Cao, L.; Massey, I.Y.; Feng, H.; Yang, F. A Review of Cardiovascular Toxicity of Microcystins. *Toxins* **2019**, *11*, 507. [[CrossRef](#)] [[PubMed](#)]
21. Shi, J.; Zhou, J.; Zhang, M. Microcystins Induces Vascular Inflammation in Human Umbilical Vein Endothelial Cells via Activation of NF-kappaB. *Mediat. Inflamm.* **2015**, *2015*, 942159. [[CrossRef](#)] [[PubMed](#)]
22. WHO. *Cyanobacterial Toxins: Microcystin-LR Guidelines for Drinking-Water Quality*; WHO: Geneva, Switzerland, 1998.
23. Komatsu, M.; Furukawa, T.; Ikeda, R.; Takumi, S.; Nong, Q.; Aoyama, K.; Akiyama, S.; Keppler, D.; Takeuchi, T. Involvement of mitogen-activated protein kinase signaling pathways in microcystin-LR-induced apoptosis after its selective uptake mediated by OATP1B1 and OATP1B3. *Toxicol. Sci.* **2007**, *97*, 407–416. [[CrossRef](#)] [[PubMed](#)]
24. Grube, M.; Kock, K.; Oswald, S.; Draber, K.; Meissner, K.; Eckel, L.; Bohm, M.; Felix, S.B.; Vogelgesang, S.; Jedlitschky, G.; et al. Organic anion transporting polypeptide 2B1 is a high-affinity transporter for atorvastatin and is expressed in the human heart. *Clin. Pharmacol. Ther.* **2006**, *80*, 607–620. [[CrossRef](#)]
25. Zhao, Y.; Xie, P.; Tang, R.; Zhang, X.; Li, L.; Li, D. In vivo studies on the toxic effects of microcystins on mitochondrial electron transport chain and ion regulation in liver and heart of rabbit. *Comp. Biochem. Physiol. C Toxicol. Pharmacol.* **2008**, *148*, 204–210. [[CrossRef](#)] [[PubMed](#)]
26. Chen, L.; Giesy, J.P.; Xie, P. The dose makes the poison. *Sci. Total Environ.* **2018**, *621*, 649–653. [[CrossRef](#)] [[PubMed](#)]
27. Zhang, X.; Zhou, C.; Li, W.; Li, J.; Wu, W.; Tao, J.; Liu, H. Vitamin C Protects Porcine Oocytes From Microcystin-LR Toxicity During Maturation. *Front. Cell Dev. Biol.* **2020**, *8*, 582715. [[CrossRef](#)]
28. Milutinović, A.; Zorc-Pleskovic, R.; Petrovic, D.; Zorc, M.; Suput, D. Microcystin-LR induces alterations in heart muscle. *Folia Biol.* **2006**, *52*, 116–118.
29. Alosman, M.; Cao, L.; Massey, I.Y.; Yang, F. The lethal effects and determinants of microcystin-LR on heart: A mini review. *Toxin Rev.* **2020**, *40*, 517–526. [[CrossRef](#)]
30. Du, C.; Zheng, S.; Yang, Y.; Feng, X.; Chen, J.; Tang, Y.; Wang, H.; Yang, F. Chronic exposure to low concentration of MC-LR caused hepatic lipid metabolism disorder. *Ecotoxicol. Environ. Saf.* **2022**, *239*, 113649. [[CrossRef](#)]
31. Qiu, T.; Xie, P.; Liu, Y.; Li, G.; Xiong, Q.; Hao, L.; Li, H. The profound effects of microcystin on cardiac antioxidant enzymes, mitochondrial function and cardiac toxicity in rat. *Toxicology* **2009**, *257*, 86–94. [[CrossRef](#)]
32. Martins, N.D.; Yunes, J.S.; McKenzie, D.J.; Rantin, F.T.; Kalinin, A.L.; Monteiro, D.A. Microcystin—LR exposure causes cardiorespiratory impairments and tissue oxidative damage in trahira, *Hoplias malabaricus*. *Ecotoxicol. Environ. Saf.* **2019**, *173*, 436–443. [[CrossRef](#)] [[PubMed](#)]
33. Saraf, S.R.; Frenkel, A.; Harke, M.J.; Jankowiak, J.G.; Gobler, C.J.; McElroy, A.E. Effects of Microcystis on development of early life stage Japanese medaka (*Oryzias latipes*): Comparative toxicity of natural blooms, cultured *Microcystis* and microcystin-LR. *Aquat. Toxicol.* **2018**, *194*, 18–26. [[CrossRef](#)] [[PubMed](#)]
34. Qi, M.; Dang, Y.; Xu, Q.; Yu, L.; Liu, C.; Yuan, Y.; Wang, J. Microcystin-LR induced developmental toxicity and apoptosis in zebrafish (*Danio rerio*) larvae by activation of ER stress response. *Chemosphere* **2016**, *157*, 166–173. [[CrossRef](#)] [[PubMed](#)]

35. Suput, D.; Zorc-Pleskovic, R.; Petrovic, D.; Milutinović, A. Cardiotoxic injury caused by chronic administration of microcystin-YR. *Folia Biol.* **2010**, *56*, 14–18.
36. Ma, Z.G.; Yuan, Y.P.; Wu, H.M.; Zhang, X.; Tang, Q.Z. Cardiac fibrosis: New insights into the pathogenesis. *Int. J. Biol. Sci.* **2018**, *14*, 1645–1657. [[CrossRef](#)]
37. Talman, V.; Ruskoaho, H. Cardiac fibrosis in myocardial infarction—from repair and remodeling to regeneration. *Cell Tissue Res.* **2016**, *365*, 563–581. [[CrossRef](#)]
38. Medeiros, N.I.; Gomes, J.A.S.; Correa-Oliveira, R. Synergic and antagonistic relationship between MMP-2 and MMP-9 with fibrosis and inflammation in Chagas' cardiomyopathy. *Parasite Immunol.* **2017**, *39*, e12446. [[CrossRef](#)]
39. Zhabyeyev, P.; McLean, B.; Patel, V.B.; Wang, W.; Ramprasath, T.; Oudit, G.Y. Dual loss of PI3Kalpha and PI3Kgamma signaling leads to an age-dependent cardiomyopathy. *J. Mol. Cell. Cardiol.* **2014**, *77*, 155–159. [[CrossRef](#)]
40. Yang, K.C.; Ku, Y.C.; Lovett, M.; Nerbonne, J.M. Combined deep microRNA and mRNA sequencing identifies protective transcriptomal signature of enhanced PI3Kalpha signaling in cardiac hypertrophy. *J. Mol. Cell. Cardiol.* **2012**, *53*, 101–112. [[CrossRef](#)]
41. McMullen, J.R.; Amirahmadi, F.; Woodcock, E.A.; Schinke-Braun, M.; Bouwman, R.D.; Hewitt, K.A.; Mollica, J.P.; Zhang, L.; Zhang, Y.; Shioi, T.; et al. Protective effects of exercise and phosphoinositide 3-kinase(p110alpha) signaling in dilated and hypertrophic cardiomyopathy. *Proc. Natl. Acad. Sci. USA* **2007**, *104*, 612–617. [[CrossRef](#)]
42. Ma, Z.G.; Yuan, Y.P.; Zhang, X.; Xu, S.C.; Wang, S.S.; Tang, Q.Z. Piperine Attenuates Pathological Cardiac Fibrosis Via PPAR-gamma/AKT Pathways. *EBioMedicine* **2017**, *18*, 179–187. [[CrossRef](#)]
43. Wei, W.Y.; Ma, Z.G.; Xu, S.C.; Zhang, N.; Tang, Q.Z. Pioglitazone Protected against Cardiac Hypertrophy via Inhibiting AKT/GSK3beta and MAPK Signaling Pathways. *PPAR Res.* **2016**, *2016*, 9174190. [[CrossRef](#)] [[PubMed](#)]
44. Sekulić, A.; Hudson, C.C.; Homme, J.L.; Yin, P.; Otterness, D.M.; Karnitz, L.M.; Abraham, R.T. A direct linkage between the phosphoinositide 3-kinase-AKT signaling pathway and the mammalian target of rapamycin in mitogen-stimulated and transformed cells. *Cancer Res.* **2000**, *60*, 3504–3513.
45. Yano, N.; Tseng, A.; Zhao, T.C.; Robbins, J.; Padbury, J.F.; Tseng, Y.T. Temporally controlled overexpression of cardiac-specific PI3Kalpha induces enhanced myocardial contractility—A new transgenic model. *Am. J. Physiol. Heart Circ. Physiol.* **2008**, *295*, H1690–H1694. [[CrossRef](#)]
46. Abeyrathna, P.; Su, Y. The critical role of Akt in cardiovascular function. *Vasc. Pharmacol.* **2015**, *74*, 38–48. [[CrossRef](#)]
47. Nagoshi, T.; Matsui, T.; Aoyama, T.; Leri, A.; Anversa, P.; Li, L.; Ogawa, W.; del Monte, F.; Gwathmey, J.K.; Grazette, L.; et al. PI3K rescues the detrimental effects of chronic Akt activation in the heart during ischemia/reperfusion injury. *J. Clin. Investig.* **2005**, *115*, 2128–2138. [[CrossRef](#)] [[PubMed](#)]
48. Mitra, A.; Luna, J.I.; Marusina, A.I.; Merleev, A.; Kundu-Raychaudhuri, S.; Fiorentino, D.; Raychaudhuri, S.P.; Maverakis, E. Dual mTOR Inhibition Is Required to Prevent TGF-beta-Mediated Fibrosis: Implications for Scleroderma. *J. Investig. Dermatol.* **2015**, *135*, 2873–2876. [[CrossRef](#)]
49. Liu, J.; Wang, H.; Wang, B.; Chen, T.; Wang, X.; Huang, P.; Xu, L.; Guo, Z. Microcystin-LR promotes proliferation by activating Akt/S6K1 pathway and disordering apoptosis and cell cycle associated proteins phosphorylation in HL7702 cells. *Toxicol. Lett.* **2016**, *240*, 214–225. [[CrossRef](#)] [[PubMed](#)]
50. Chen, Y.; Wang, J.; Pan, C.; Li, D.; Han, X. Microcystin-leucine-arginine causes blood-testis barrier disruption and degradation of occludin mediated by matrix metalloproteinase-8. *Cell. Mol. Life Sci.* **2018**, *75*, 1117–1132. [[CrossRef](#)]
51. Zhou, Y.; Sun, M.; Tang, Y.; Chen, Y.; Zhu, C.; Yang, Y.; Wang, C.; Yu, G.; Tang, Z. Responses of the proteome in testis of mice exposed chronically to environmentally relevant concentrations of Microcystin-LR. *Ecotoxicol. Environ. Saf.* **2020**, *187*, 109824. [[CrossRef](#)]

Disclaimer/Publisher's Note: The statements, opinions and data contained in all publications are solely those of the individual author(s) and contributor(s) and not of MDPI and/or the editor(s). MDPI and/or the editor(s) disclaim responsibility for any injury to people or property resulting from any ideas, methods, instructions or products referred to in the content.